Estuaries and Coasts (2023) 46:404–416
https://doi.org/10.1007/s12237-022-01138-x

The Role of Invasive *Phragmites australis* in Wave Attenuation in the Eastern United States

Daniel J. Coleman[1] · Felicio Cassalho[1] · Tyler W. Miesse[1] · Celso M. Ferreira[1]

Received: 25 January 2022 / Revised: 15 September 2022 / Accepted: 17 October 2022 / Published online: 27 October 2022

Abstract

In much of the USA, *Phragmites australis* is a prolific invasive species in wetland habitats. The spread of *Phragmites* can significantly alter the structure and function of a marsh, thereby altering the ecosystem services that the marsh provides. It remains unclear how *Phragmites* invasion may impact coastal protection, despite the substantial implications for local communities. Here, we investigated the ability of a *Phragmites* marsh to attenuate waves via long-term field monitoring and compared this to native *Spartina alterniflora* via hydrodynamic modeling. *Phragmites* was capable of attenuating incoming waves and did so most effectively at higher stem densities and lower water levels. Under no conditions studied here did *Phragmites* attenuate waves more than *S. alterniflora*. During the summer and fall as well as during lower water levels, *Phragmites* significantly underperformed *S. alterniflora*. This indicates that *Phragmites* invasion may conditionally increase the coastal hazard facing local communities, and highlights that *Phragmites* management should be coupled with the restoration of native species.

Keywords Salt marsh · Wave attenuation · Phragmites · Field study · Hydrodynamic model

Introduction

Storm surge and waves can be devastating to coastal communities, but the impact can be mitigated by coastal wetlands. By acting as a buffer, coastal wetlands reduce storm surge and attenuate waves (Loder et al. 2009; Möller et al. 2014; Vuik et al. 2016; Glass et al. 2018; Paquier et al. 2017; Garzon et al. 2019a, b). These crucial habitats offer many ecosystem services in addition to coastal protection, such as nursery habitat for nesting birds and commercially important fisheries (Deegan et al. 2002; Norris et al. 2004), water filtration (Barbier et al. 2011), and carbon sequestration (Chmura et al. 2003). The value of coastal wetlands is underscored by their vulnerability to environmental change, such as sea-level rise and invasive species. When the structure and function of natural wetlands is significantly altered, their ability to provide ecosystem services can be lost.

One invasive species that is prolific in US wetlands is *Phragmites australis*. The non-native genotype of *Phragmites australis* (hereafter referred to as *Phragmites*) has rapidly expanded and even extirpated the native subspecies, *Phragmites australis americanus*, from entire regions (Saltonstall 2002). In many wetlands, diverse assemblages of native plants are replaced by a monoculture of *Phragmites* (Silliman and Bertness 2004). This replacement is associated with a decrease in plant biodiversity and an alteration of vertebrate and invertebrate communities (Chambers et al. 1999; Weinstein and Balletto 1999; Angradi et al. 2001; Meyer et al. 2010). This means the invasion of *Phragmites* can reduce the ability of the wetland to provide certain ecosystem services, such as offering nursery habitat.

Interestingly, *Phragmites* can also enhance certain other ecosystem services associated with wetlands. For example, *Phragmites* may enhance wetland water filtration, as it reduces the bioavailability of toxic metals mercury, chromium, and lead more so than *S. alterniflora* (Windham et al. 2003). Additionally, *Phragmites* can accrete sediment more rapidly than native wetland species (Rooth and Stevenson 2000; Rooth et al. 2003; Langston et al. 2021), which is crucial for the ability of a wetland to survive sea-level rise. Management efforts

Communicated by John C. Callaway.

✉ Daniel J. Coleman
daniel.coleman@uga.edu

[1] Volgenau School of Information Technology and Engineering, Department of Civil, Environmental, and Infrastructure Engineering, George Mason University, Fairfax, USA

to remove *Phragmites* could therefore be detrimental to the persistence of particular marshes and the communities that rely on them.

One ecosystem service that has been under studied with respect to *Phragmites* invasion is coastal protection. Wave attenuation in coastal marshes is related to characteristics of the vegetation, such as stem height, stem thickness, and stem density (Anderson and Smith 2014; Maza et al. 2015; Garzon et al. 2019b; Xue et al. 2021). Different plant species have different capabilities to attenuate waves (Xue et al. 2021). Given that *Phragmites* differs from native vegetation in these biometric characteristics, it can be expected that the ability of a *Phragmites*-dominated marsh to attenuate waves will also differ from native marshes. A previous modeling study demonstrates that *Phragmites* and native *Typha* would have offered similar wave protection during Super Storm Sandy at a marsh in New York, USA (Sheng et al. 2021). Additionally, the authors note that had Sandy occurred outside of the growing season, the *Phragmites* marsh would have outperformed the shorter and sparser native vegetation (Sheng et al. 2021). While this study demonstrates the usefulness of modeling to compare *Phragmites* to native vegetation and that *Phragmites* can protect coastal communities during major storms, additional questions remain. For instance, there is a lack of field-based evidence of wave attenuation potential by *Phragmites* and how this potential compares to other native species, such as *Spartina alterniflora*. Furthermore, it is unclear what factors most control wave attenuation by *Phragmites* outside of major hurricanes. With climate change, humans will likely experience greater coastal hazards (Collins et al. 2019) making it particularly important to understand how *Phragmites* invasion will impact coastal protection.

Here we explored these questions through a long-term, field-monitoring study in a *Phragmites*-dominated wetland in the Chesapeake Bay, USA, combined with a calibrated, numerical model. We measured waves and water levels every 10 min for approximately 12.5 months and paired these measurements with seasonal measurements of stem height, stem thickness, and stem density. From this unique, high-resolution record, we calculated how waves changed across the marsh platform and what factors influenced these changes. We then compared wave attenuation in non-native *Phragmites* to native *S. alterniflora* using a numerical model. This allowed us to account for extraneous differences between the study site and a *S. alterniflora*-dominated reference site, as well as incorporate extreme conditions not observed during the monitoring window. This work represents one of the first field-based analyses of wave attenuation in *Phragmites*, as well as a comparison study between *Phragmites* and native *S. alterniflora*. Our findings will have implications for the management of this prodigious invasive species and coastal wetland restoration.

Methods

Field Measurements

This study was conducted at Franklin Point State Park, Maryland, USA, at a *Phragmites*-dominated marsh on the mainstem of the Chesapeake Bay (Fig. 1). The system as a whole is erosional, as evidenced by a small marsh escarpment and numerous downed trees in the water south of the site. The spring tidal range is approximately 0.5 m, and the site experiences regular wave activity. From August 2020 to August 2021, we maintained a shore-normal transect of pressure gauges (RBR brand D-Wave solo3). The sensors have an initial measurement threshold of 1 cm and a resolution less than 0.02 cm (https://rbr-global.com/products/compact-loggers/compact-tide-wave). We visited the site periodically to clean, download, and redeploy the sensors. We utilized four sensors, one located in the water just offshore of the marsh (sensor 1, 4.29 m from the marsh edge, average water depth of 0.56 m) and three located progressively interior on the intertidal marsh platform (sensors 2, 3, and 4, 0.71 m, 3.21 m, and 6.21 m from the marsh edge, respectively). The sensors were mounted to fence posts that were driven into the substrate. The point of measurement for the sensors on the marsh was located within 4 cm of the marsh platform, and for the sensor in the water, it was located 13 cm from the bed.

The wave sensors measured pressure every 10 min with a 1024 count, a 4-Hz burst for the duration of the deployment. This produced a time series of pressure which we then converted to water depth by subtracting atmospheric pressure measured at a nearby National Oceanographic and Atmospheric Administration (NOAA) buoy. From the pressure time series, we calculated numerous wave parameters of interest, including the significant wave height of each measurement burst, using the Ruskin software (https://docs.rbr-global.com/support/ruskin). Wave statistics were determined via the zero up-crossing approach. In the pressure and significant wave height time series, we removed all timesteps for which pressure was less than or equal to zero, which corresponds to times the sensor was not flooded, and all timesteps when waves were less than 1 cm, which is the detection limit of the instruments. During the deployment, there were equipment issues that resulted in missing data during the fall of 2020, especially at the offshore sensor.

We measured stem height, stem thickness, and stem density at each sensor location seasonally to characterize the vegetation affecting wave attenuation (Supplemental Fig. 1). Vegetation was measured on August 8, 2020, November 23, 2020, February 5, 2021, May 13, 2021, and August 25, 2021. We randomly placed four 0.25 m × 0.25 m subplots within an approximately 0.75-m radius circle centered on the

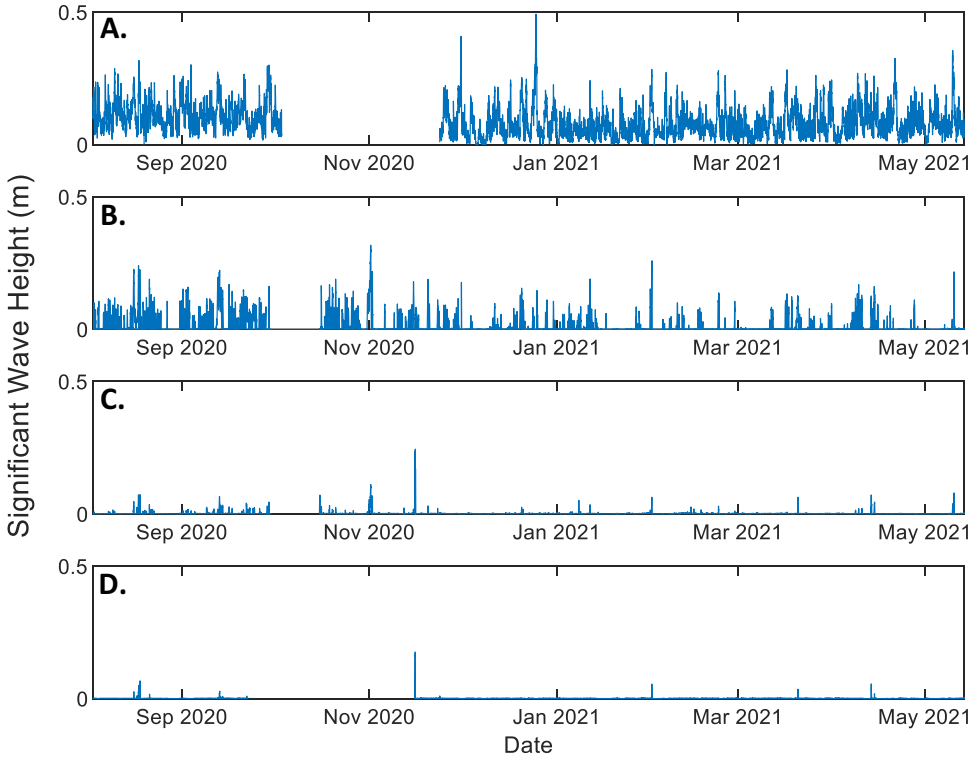

Fig. 1 Time series of significant wave height for **A** sensor 1 (the offshore sensor), **B** sensor 2, **C** sensor 3, and **D** sensor 4 (the farthest interior sensor). Note the gaps in data during the fall of 2020, with the largest gap in the offshore sensor

marsh sensor, and we repeated this for each marsh sensor. In each subplot, we counted all standing stems to calculate density as number of stems per square meter. We measured the height of five random plants in the subplot using a measuring tape. Similarly, we measured the diameter of five random plants using digital calipers. Average density was calculated for each sensor by averaging the four corresponding subplots while average height and diameter was first calculated for a subplot, and then for the sensor. As such, the standard deviation for stem height and diameter for a given sensor was calculated as the square root of the sum of the squared subplot-level standard deviations.

We conducted a GPS survey of the site to quantify the topography and bathymetry as these parameters also play an important role in wave attenuation (see Fig. 5). We used a Trimble R4 real-time kinematic GPS on both the marsh platform and the shallow water offshore (error < 0.02 m in elevation).

In parallel to this *Phragmites*-dominated marsh, we also monitored a reference site that was dominated by *S. alterniflora* and located within the Blackwater National Wildlife Refuge (Lat: 38° 13′ 34″ N Long: 76° 02′ 39″ W). We used the same methodology described above to quantify wave height, water level, vegetation characteristics, and topography/bathymetry. Pressure monitoring was conducted from late September 2020 to mid-May 2021 and vegetation surveys were conducted on August 20, 2020, November 23, 2020, February 5, 2021, May 13, 2021, and August 25, 2021. Sensor 1 was located 2.81 m from the marsh edge in an average water depth of 0.46 m and sensors 2–4 were located on the intertidal marsh platform at 2.29 m, 8.84 m, and 15.60 m from the marsh edge, respectively.

Analytical Methods

To represent wave attenuation by *Phragmites*, we calculated the change in wave height with distance for each 10-min increment for the duration of the study. Since wave height has been shown to decay exponentially with distance into the wetland (Massel et al. 1999; Möller et al. 2014; Vuik et al. 2016; Paquier et al. 2017; Foster-Martinez et al. 2018; Garzon et al. 2019a; Xue et al. 2021), we used the following equation.

$$H(x) = H_0 * e^{kx} \quad (1)$$

Here, H represents significant wave height, x is the distance into the marsh, H_0 is the significant wave height at $x = 0$, and k is the coefficient of decay. We set the marsh edge to be equal to 0 m, such that the offshore sensor had a negative distance (−4.29 m) and the sensors on the marsh platform have positive distances (0.71 m, 3.21 m, and 6.21 m). We calculated the y-intercept and slope of the line fit to the natural log of the significant wave height at each sensor location versus the sensor distance. The slope of this line equals k and the natural log of the y-intercept equals H_0. Wave height will always decrease to 0 m where the flooding depth

is also 0 m. We focused on wave attenuation by vegetation, so we excluded the offshore sensor from our analysis, as well as all time increments when the farthest interior (and highest elevation) sensor is not flooded. Once we calculated Eq. (1) for every measurement time that fit our criteria ($n = 167$, or 0.4% of time increments), we averaged H_0 and k for this full set of measurements and for only the times with the highest 10% of significant wave heights recorded at the offshore sensor. Additionally, we calculated H_0 and k using Eq. 1 for the reference, *S. alterniflora*-dominated site for measurement times meeting the same criteria ($n = 169$, or 0.4% of time increments).

We separated the time series into bins based on water level and wave height to further investigate the role these parameters have in controlling wave attenuation rate. Specifically, we used the water level and wave height recorded at the farthest interior sensor (sensor 4) as the variables defining the bins. First, each time increment was classified as having an initial water level that was in the lowest third of the measurements (< 0.027 m), the middle third (0.027–0.056 m), or the highest third (> 0.056 m). We compared the decay coefficient, k, and initial wave height at the offshore sensor via linear regression for each water level bin. Next, we repeated this process, but binned the timesteps by wave height rather than water level. Again, we grouped the measurements into the lowest third (< 0.024 m), middle third (0.024–0.034 m), and highest third (> 0.034 m). We then compared the decay coefficient, k, and initial water level at the offshore sensor via linear regression for each wave height bin.

To determine the effect of vegetation on wave attenuation, we created linear regressions between vegetation characteristics and the decrease in wave height at the same location on the marsh. First, we created time histories of the percent decrease in wave height from one sensor to the next farther inland sensor. Because this analysis only required data to be available at two consecutive sensors, we included time increments that did not meet the criteria for the analysis of wave height decay (such as time increments when only sensor 1 and sensor 2 were flooded). We divided the time histories such that a given period contained all of the time increments closer to one vegetation sampling date than another. For example, all wave data recorded between the start of the study and October 6, 2020 (the halfway point between the first and second vegetation sampling dates) were grouped into the first period. Wave data recorded after October 6, 2020, up until the next dividing date was grouped into the second period. We then averaged the percent decrease in wave height for these periods, and compared them to the vegetation characteristics measured at the central date. Specifically, we compared the percent decrease between sensor A and sensor B to the vegetation characteristic measured at sensor B. From this, we created linear regressions comparing percent decrease in wave height to each vegetation characteristic (stem height, stem thickness, and stem density), utilizing the maximum amount of data from across the marsh platform and over the sampling duration.

Modeling Approach

We used the public-domain, numerical model Xbeach to simulate wave propagation onto two theoretical marsh platforms: one composed of *Phragmites* and the other of *Spartina alterniflora*. The model solved short-wave motion across a 1-dimensional cross section that extends from the open water to the marsh interior using the wave action equation (van Rooijen et al. 2015). A wave boundary condition is applied at the open water end of the model using a JONSWAP spectrum. The waves then propagate across the marsh platform, and the model calculates changes in wave height caused by interactions with the topography (bottom friction) and vegetation. The coefficient of drag (C_D) was calculated based on hydrodynamic conditions, as defined by Garzon et al. (2019a, b). The topography and cross-sectional length for both theoretical marsh platforms used here was defined using the RTK GPS surveys of the Franklin Point field site. The vegetation in Xbeach is approximated as rigid cylinders of specified density, height, and diameter. We used the average stem density, stem height, and stem diameter measurements from all samples from within the Franklin Point marsh interior (proximal to sensors 3 and 4) to define these characteristics for the theoretical *Phragmites* marsh. Additionally, we conducted a model validation comparing this average vegetation characteristic approach to spatially varying vegetation. The vegetation of the theoretical *S. alterniflora* marsh was defined via vegetation surveys at the *S. alterniflora*-dominated marsh. For this study, we utilized the Xbeach wave-breaking model (Roelvink et al. 2009; Daly et al. 2012) and did not allow for geomorphic changes. The spatial resolution varied from 1.5 m at the open water end of the cross section to 0.25 m at the marsh interior end.

We ran an array of model simulations to compare *Phragmites* and *S. alterniflora* under different wave height and water level conditions. For each set of conditions, we ran the model using the average of each of the three vegetation characteristics for the two plant species. Additionally, we defined a confidence interval as a model simulation using the average minus the standard error for each of the three vegetation characteristics as the lower bound and a simulation using the average plus the standard error for each of the three vegetation characteristics as the upper bound. The values for the vegetation characteristics used to represent each species and the associated standard errors can be found in Table 1. For the first model simulation, we used an initial wave height that represented the average of the top 10% of waves recorded at the offshore sensor (0.29 m), then

rounded for simplicity (0.3 m). This was then paired with the water level that was observed at the same time waves of this height were observed (0.75 m). This first simulation therefore represents the higher end of observed conditions, and since there was no major storm or hurricane over the monitoring period, it represents the higher end of common or "everyday" conditions. We then conducted a series of simulations using vegetation characteristics representative of each season, using these same wave height and water level conditions. The vegetation characteristics for each season were defined by the survey or surveys that occurred closest to the end of that season (Table 1). For example, the spring simulation used vegetation characteristics for *Phragmites* determined from the May 13, 2021, survey and *S. alterniflora* from the May 18, 2021, survey.

To determine how waves would be attenuated by the different species under extreme conditions, we used a 3×3 factorial design, varying wave height and water level. The wave height values used were 0.3 m, 0.6 m, and 1 m, and the water levels used were 0.75 m, 1.4 m, and 2.0 m. The water level values were specifically chosen such that neither plant species would be submerged by the low value, only *S. alterniflora* would be submerged by the middle value, and both plant species would be submerged by the high value. Additionally, our highest water level (2.0 m) is similar to the highest water level recorded at the nearby Annapolis, MD tide gauge since it was established in 1978, which was 1.96 m during Hurricane Isabel (www.tidesandcurrents.noaa.gov). This factorial design allows for a more complete comparison of *Phragmites* and *S. alterniflora* under a range of conditions.

Results

Field-Based Results

Significant wave height decreased with distance into the marsh (Fig. 1). The more inland locations had lower wave heights and fewer wave events than the location in the water or at the marsh edge, which can partially be explained by less frequent flooding in the interior. The maximum significant wave height observed at the offshore sensor was 0.49 m, the median height was 0.06 m, and 57% of time increments had wave heights greater than 0.05 m. In contrast, the maximum significant wave height at the most inland location was 0.18 m, the median height was 0 m, and 0.05% of time increments had wave heights greater than 0.05 m. At the reference, *S. alterniflora*-dominated site, the maximum significant wave height for the offshore sensor was 0.20 m, the median height was 0.02 m, and 14.8% of time increments had wave heights greater than 0.05 m.

Table 1 Values for the vegetation characteristics used to represent each species for the seasonal and overall analyses (average of all vegetation surveys)

		Density (#/m^2)	Height (cm)	Diameter (mm)
Phragmites	Summer	**273**	**172.9**	**5.36**
	8/20/2020 and 8/25/2021	34.64	7.16	0.192
	Fall	**178**	**72.5**	**4.64**
	11/23/2020	22.10	10.61	0.255
	Winter	**176**	**53.8**	**4.94**
	2/5/2021	27.05	10.44	0.294
	Spring	**292**	**122**	**5.47**
	5/13/2021	29.59	4.94	0.263
	All-survey average	**238.4**	**116.3**	**5.14**
		18.04	5.50	0.120
Spartina alterniflora	Summer	**1040**	**70.7**	**3.09**
	9/28/2020 and 7/21/2021	368.95	4.78	0.358
	Fall	**1892**	**75.4**	**2.02**
	11/12/2020	922.98	7.65	0.290
	Winter	**396**	**62.9**	**2.67**
	3/18/2021	172.37	5.43	0.389
	Spring	**608**	**25.6**	**2.98**
	5/18/2021	194.54	1.99	0.521
	All-survey average	**771.4**	**65.7**	**3.05**
		230.23	3.93	0.210

Bold values indicate the average and non-bold indicate the standard errors, which were used to calculate confidence intervals (i.e. ± 1 s.e.). The dates indicate when the survey or surveys that were included in each season were conducted

The decrease in significant wave height with distance into the marsh was exponential in nature (Fig. 2). When including all time steps when data were available at each marsh sensor, the equation to describe change in wave height with distance can be given as:

$$H(x) = 0.22\ (\pm 7.1 * 10^{-3}) * e^{-0.22\ (\pm 5.7 * 10^{-3})\ x} \quad (2)$$

where the number in parentheses represents one standard error. When using only the times representing the highest 10% of significant wave heights recorded at the offshore sensor, the equation is instead given as:

$$H(x) = 0.29\ (\pm 7.1 * 10^{-3}) * e^{-0.25\ (\pm 0.011)\ x} \quad (3)$$

Under both conditions, significant wave height decreased rapidly within the first several meters of the marsh platform. For the reference, *S. alterniflora*-dominated site, the wave attenuation equation calculated using all time increments when the marsh interior sensor was flooded by at least one centimeter ($n = 169$) is given as:

$$H(x) = 0.03\ (\pm 6.6 * 10^{-3}) * e^{-0.12\ (\pm 0.012)\ x} \quad (4)$$

Water level and wave height had a significant effect on wave attenuation rate, as defined by the decay coefficient, k (Fig. 3). For a given wave height class, the decay coefficient, k, increased as the water level increased (Fig. 3a). This indicates that there was less wave attenuation at higher water levels. For a given water level class, the decay coefficient, k, decreased as the initial wave height increased, indicating there was greater wave attenuation at higher wave heights (Fig. 3B). The slope of the relationship between water level and the decay coefficient, k, was very similar for all wave height bins (lowest third: $k = 0.51$ * water level $- 0.71$, $p < 0.01$, $R^2 = 0.28$, $n = 57$; middle third: $k = 0.52$ * water level $- 0.69$, $p < 0.01$, $R^2 = 0.60$, $n = 56$; highest third: $k = 0.55$ * water level $- 0.67$, $p < 0.01$, $R^2 = 0.65$, $n = 54$; Fig. 3A). Similarly, the slope of the relationship between wave height and the decay coefficient, k, was very similar for all water level bins (lowest third: $k = -0.63$ * wave height $- 0.13$, $p < 0.01$, $R^2 = 0.32$, $n = 33$; middle third: $k = -0.65$ * wave height $- 0.12$, $p < 0.01$, $R^2 = 0.43$, $n = 59$; highest third: $k = -0.46$ * wave height $- 0.09$, $p < 0.01$, $R^2 = 0.23$, $n = 58$; Fig. 3B). In other words, both the relationship between wave attenuation and water level, as well as wave attenuation and initial wave height were fairly constant under the range of observed conditions.

The percent decrease in wave height from one sensor to the next sensor was significantly related to stem density, marginally significantly related to stem diameter but not significantly related to stem height (Fig. 4). The percent decrease in wave height between adjacent sensors increased as stem density increased ($R^2 = 0.36$, $p < 0.05$, $n = 15$), but decreased as stem diameter increased ($R^2 = 0.19$, $p < 0.1$, $n = 15$). Stem density and stem diameter covaried and were

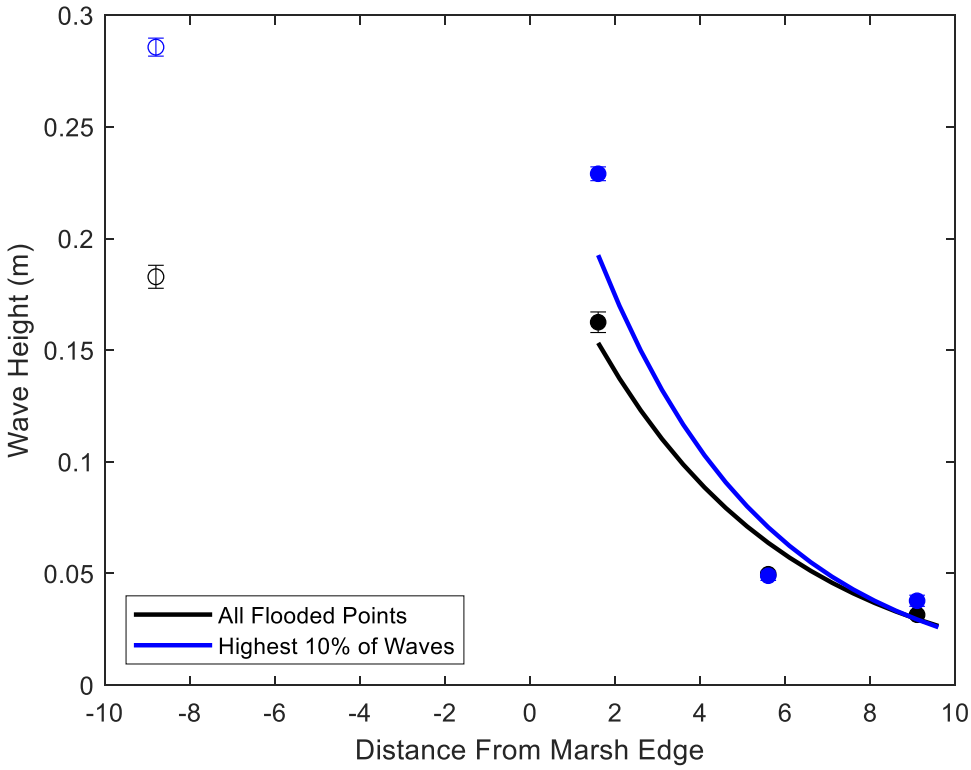

Fig. 2 Wave attenuation within the marsh at all times when the marsh sensors were all flooded (black) and only times that represent the highest 10% of waves at the offshore sensor (blue). Error bars represent ± one standard error. The points represent the average wave height for each sensor under the specified conditions, with the open point indicating the average wave height at the offshore sensor, which is not included in the calculation of the attenuation curve. Note that the black point at 5.6 m is behind the blue point at this distance

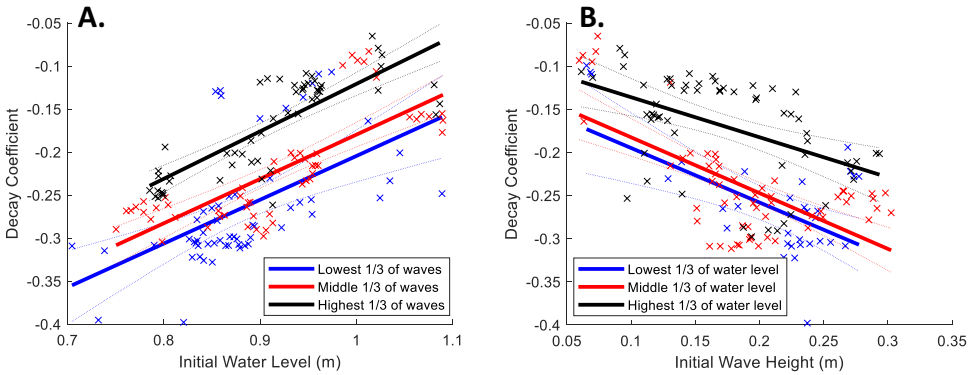

Fig. 3 **A** Relationship between the water level at the offshore sensor and the decay coefficient (k in Eq. 1), grouped by bins of initial wave height. For a given range of wave heights, wave attenuation decreases with increasing water depth. **B** Relationship between the initial wave height at the offshore sensor and the decay coefficient (k in Eq. 1), grouped by bins of initial water level. For a given range of water depths, wave attenuation increases with increasing wave height

inversely correlated ($R^2 = 0.29$, $p < 0.05$, $n = 15$). While stem height covaried with both stem density ($R^2 = 0.41$, $p < 0.05$, $n = 15$) and stem diameter ($R^2 = 0.24$, $p < 0.1$, $n = 15$), it was not significantly related to the percent decrease in wave height between adjacent sensors ($R^2 = 0.02$, $p = 0.58$, $n = 15$).

Model Results

The modeled wave heights closely matched the observed wave heights in the *Phragmites*-dominated marsh (Fig. 5). Furthermore, the model using constant vegetation performed at least as well as the model using spatially varying vegetation (Fig. 5). This ensures that wave attenuation in our simplified, simulated marsh behaved similarly to the natural system.

Both *Phragmites* and *S. alterniflora* decreased the height of the waves traveling through the simulated marsh. The first numerical model scenarios (wave height = 0.3 m and water level = 0.75 m) were representative of the high end of observed conditions and featured wave heights that decreased rapidly with distance for both *Phragmites* and *S. alterniflora* marsh platforms (Fig. 6). For a given distance, wave height was lower in the *S. alterniflora* marsh than in the *Phragmites* marsh, especially before the wave height reached a low, fairly constant value of < 10% of the initial height. For the yearly-averaged vegetation characteristics, the difference in wave attenuation between the species was statistically significant, evidenced by the non-overlapping confidence intervals of the two plant species (Fig. 6A). Differences in seasonal biomass patterns between *Phragmites* and *S. alterniflora* resulted in seasonal differences in how the wave attenuation between the two species compared to one another (Table 1, Fig. 6). The difference in performance was most pronounced during the fall (*S. alterniflora* attenuated waves to 27% of initial wave height within 2 m, compared to 64% by *Phragmites* within 2 m, Fig. 6E), followed by the summer (S. alterniflora: 32% within 2 m, Phragmites: 52% within 2 m, Fig. 6D). There was no significant difference during the winter (both species: approximately 60% within 2 m, Fig. 6B) and spring (both species: approximately 50% within 2 m, Fig. 6C).

Changes in wave height and water level altered the ability of the vegetation to attenuate waves, as well as how the two species compared with one another. At higher wave heights (0.6 m and 1 m) and with the same water level (0.75 m), *S.*

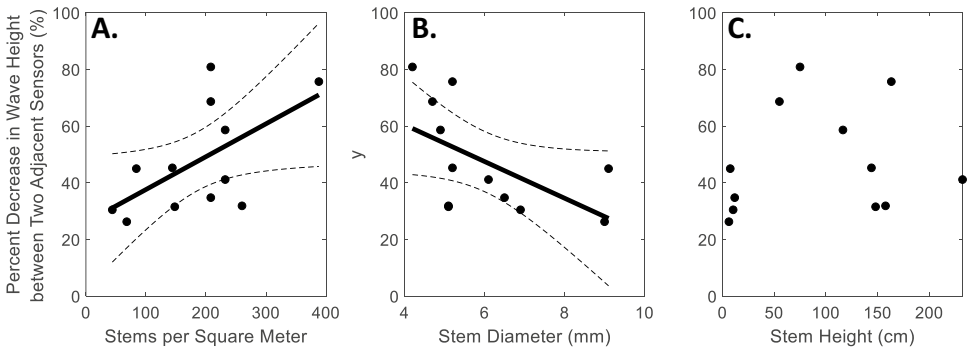

Fig. 4 The percent decrease in wave height between one sensor and the next more inland sensor computed over the time-averaging windows vs. **A** average stem density, **B** average stem diameter, and **C** average stem height. Trend line (solid line) and 95% confidence intervals (dashed line) are only included when the correlation is at least marginally significant

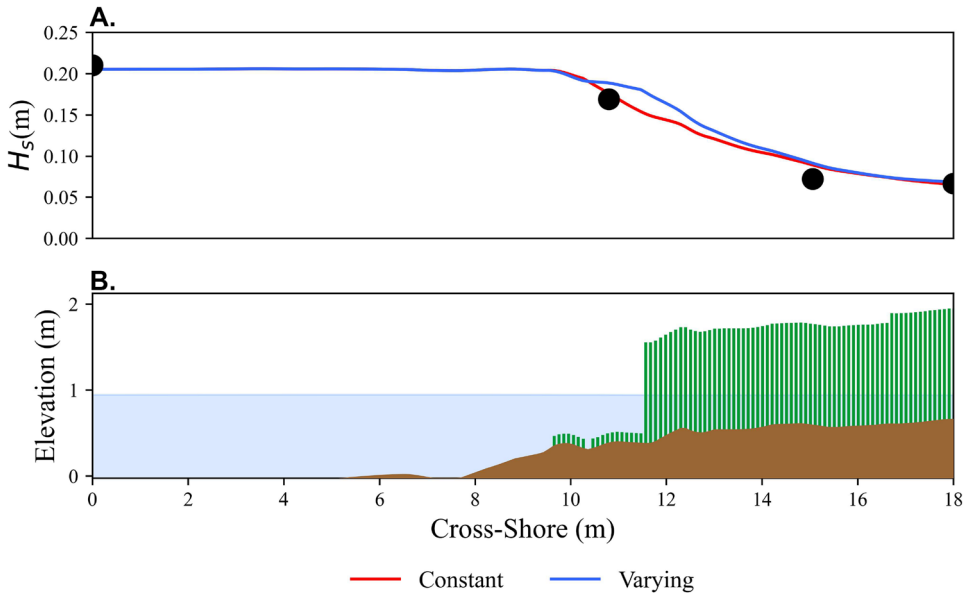

Fig. 5 **A** Numerical model simulation of significant wave height, H_S, compared to the observed wave height at the sensor locations (black circles) when taking into consideration vegetation characteristics that vary with distance along the transect (blue line) and that are held constant (red line) The C_D is calculated from hydrodynamic conditions and does not require tuning to produce these results. **B** A graphical representation of vegetation and topography with an approximate vertical exaggeration of 2×. The condition represented here occurred on August 18, 2020, at 3:00 AM local time; water level measured at the offshore sensor was 0.95 m and significant wave height was 0.21 m; and vegetation characteristics are defined by the August 20, 2020, survey

alterniflora continued to attenuate waves to a greater degree than *Phragmites* (Fig. 7). However, at higher water levels (1.4 m and 2.0 m) there was no difference in wave attenuation between *Phragmites* and *S. alterniflora*, at any of the initial wave height levels (Fig. 7). Additionally, the overall magnitude of wave attenuation decreased with increasing water level for both plant species. For example, for the same initial wave height, wave height was reduced to less than 10% within the first 6 m under the lowest water level but was only reduced to approximately 70% within the first 6 m under the highest water level (Fig. 7A, G). Under all conditions, there was significantly greater reduction of wave height with the addition of vegetation as opposed to just the bottom friction provided bare sediment, as illustrated by the difference between the black dashed line and species-specific lines in Fig. 7.

Discussion

Field Observations of Wave Attenuation in Phragmites

We observed many of the basic patterns of wave attenuation in the representative *Phragmites*-dominated marsh studied here as have been found in marshes with different vegetation. For example, average significant wave height within the marsh for all time increments when the marsh was completely flooded and the 10% highest wave conditions decayed exponentially (Fig. 2). This same exponential decay is widely described in the literature and found in marshes throughout the world (See Massel et al. 1999; Möller et al. 2014; Vuik et al. 2016; Paquier et al. 2017; Garzon et al. 2019a; Xue et al. 2021). We also noted a decrease in wave attenuation as the water level increased (Fig. 3a). Numerical-modeling and field-based studies in the Chesapeake Bay using the native *S. alterniflora* also show an inverse relationship of wave attenuation and water level (Glass et al. 2018; Paquier et al. 2017; Garzon et al. 2019a, b). Additionally, for fixed water levels and varying significant wave heights, Garzon et al. (2019b) observed that the higher the wave heights, the greater percentage decrease in wave height *S. alterniflora* provided. Similarly, we found that increases in initial wave heights lead to greater wave attenuation in the *Phragmites*-dominated marsh (Figs. 2 and 4B). This all suggests that *Phragmites*-dominated marshes are not fundamentally different than other marshes with regard to wave attenuation.

Generally, higher vegetation biomass results in a higher potential for wave attenuation (Maza et al. 2015). However, when looking at individual biomass-related vegetation characteristics, there is a significant degree of non-linearity (Xue et al. 2021). Of the three characteristics studied here (stem

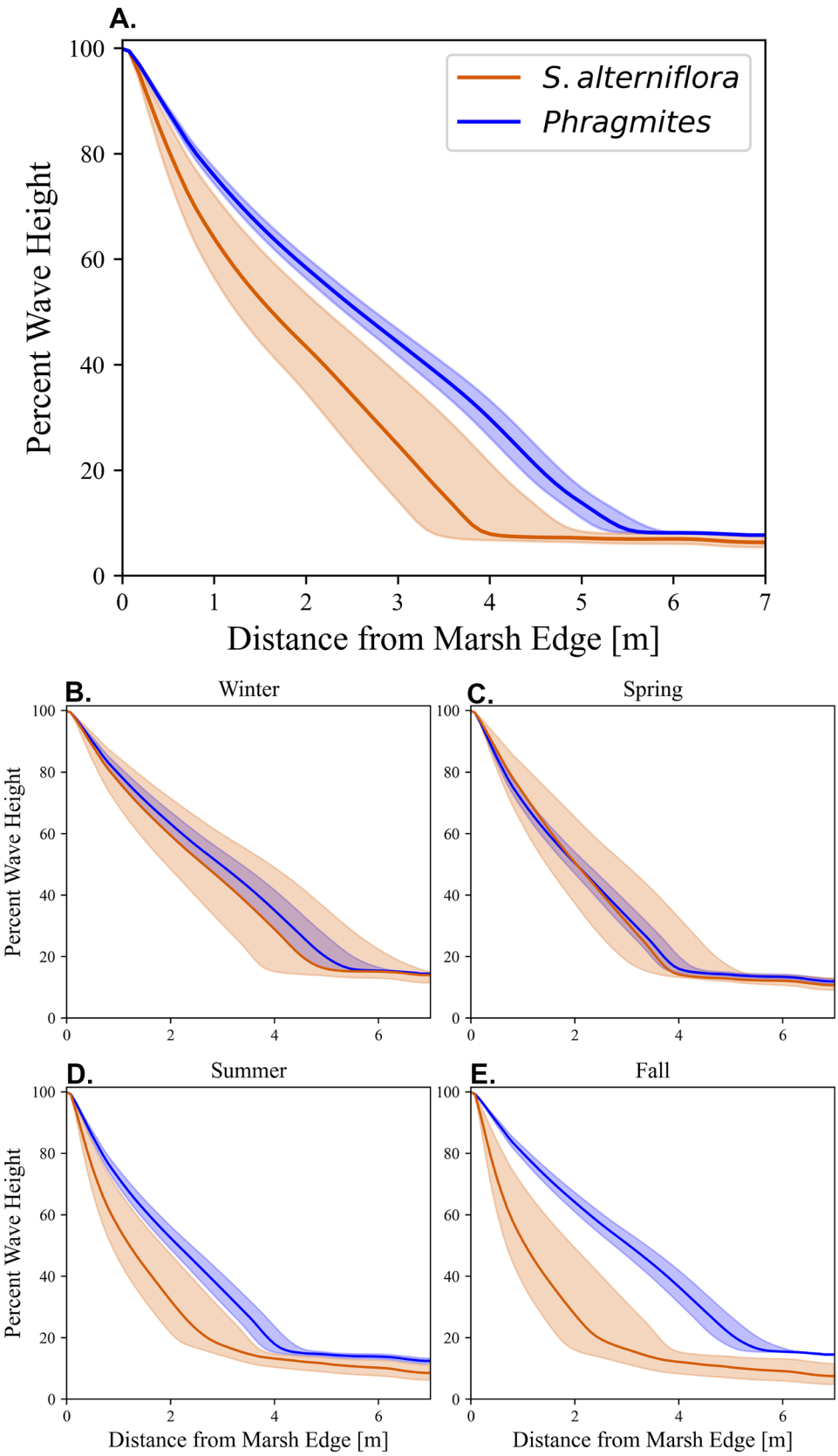

Fig. 6 Numerical model simulations (wave height = 0.3 m and water level = 0.75 m) of **A** yearly averaged vegetation characteristics of *Phragmites* (blue) and *S. alterniflora* (red) show a rapid decrease in wave height, with a more rapid decrease under conditions representative of *S. alterniflora*. Conditions representative of the individual seasons indicate no difference between wave attenuation provided by *Phragmites* and *S. alterniflora* in the **B** winter and **C** spring and pronounced differences in **D** summer and **E** fall. The lines represent model simulations using the average of each of the three vegetation characteristics. The shaded regions indicate the confidence interval, as defined in "Modeling Approach."

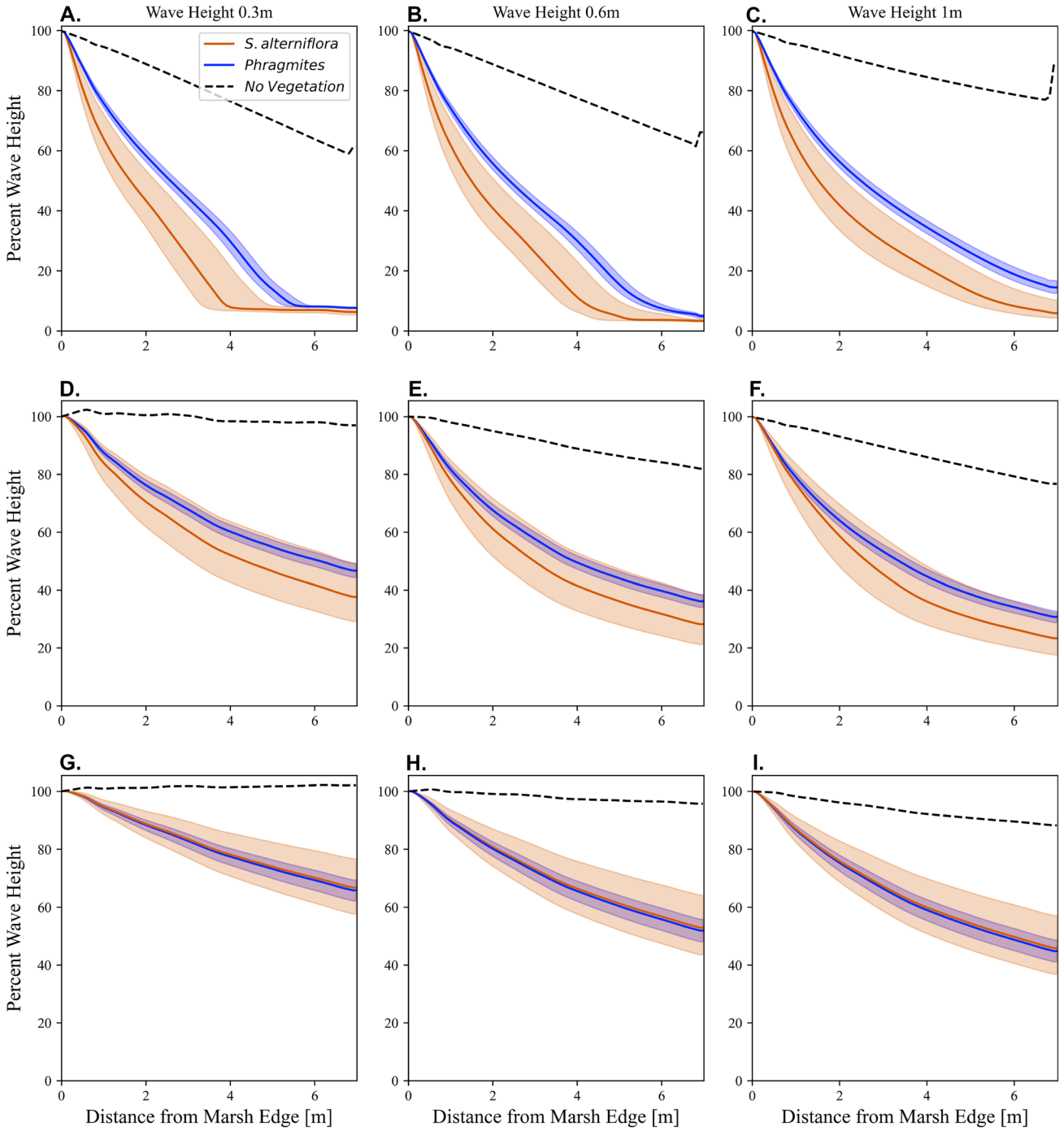

Fig. 7 Model simulations of wave attenuation for the yearly averaged *Phragmites* marsh (blue), *S. alterniflora* (red), and without vegetation (dashed line). The top graphs (**A**, **B**, **C**) represent initial water level of 0.75 m, the middle row (**D**, **E**, **F**) water level is 1.4 m, and the bottom row (**G**, **H**, **I**) water level is 2.0 m. Only under the lowest water level (**A**, **B**, **C**) is there a difference in wave attenuation between the two species of plants studied here

density, stem diameter, and stem height), previous studies have shown stem density to be the most influential on attenuation of waves, especially when the plants are not fully submerged (Anderson and Smith 2014; Maza et al. 2015). This is consistent with our findings, where stems per square meter had the strongest relationship with the decrease in wave height between sensors (Fig. 4A). Stem diameter is expected to be the least impactful characteristic on wave height reduction (Garzon et al. 2019b). We found diameter to only be marginally significantly related to the decrease in wave height between sensors (Fig. 4B). Additionally, the relationship here was inverse whereas it is expected to be

direct. Stem density and diameter were also significantly, inversely correlated. Given the expected strength of the effects of these vegetation characteristics, it is likely that wave attenuation was responding directly to stem density and the marginally significant relationship with diameter was a result of this covariance. Lastly, stem height has previously been highlighted as an important vegetation characteristic in controlling wave attenuation (Anderson and Smith 2014; Maza et al. 2015; Garzon et al. 2019a, b), However, during our year-long data-gathering campaign the vegetation was never overtopped by water and therefore, all variation in the stem height occurred outside of the area which could affect the waves. Unsurprisingly then, we did not see a correlation between height and wave attenuation (Fig. 4C).

Our study also highlights the challenges of field-based studies and the utility of modeling. In addition to sensor malfunctions, data can be sparse due to atmospheric and hydrologic conditions observed while monitoring. During the entire monitoring campaign, the marsh interior only flooded to greater than one centimeter above the sensor height (the measurement threshold for the sensors) 167 times. This represents 0.4% of measurement times and 14 flooding events. A monitoring effort at this site with less temporal resolution or a shorter timeframe may not have been able to reach the same statistical conclusions that we were able to. Additionally, the wave attenuation rate was dependent on topography and incoming wave height. It is therefore difficult to compare two marshes that differ in these parameters. For example, the interior of the *S. alterniflora*-dominated reference site flooded to the threshold depth 169 times, but incoming waves to this site were generally much lower than the *Phragmites*-dominated study site (average of 0.03 m and 0.09 m, respectively). As such, comparing the field-calculated attenuation rates between the two sites (Eqs. 3 and 4) is difficult and does not give a clear indication of the differences between these species. Modeling was therefore necessary to control for incoming wave height and topography. Modeling also allowed us to predict the ability of marshes dominated by either species to attenuate waves under conditions not observed during this monitoring year.

Model Comparison of Wave Attenuation in Phragmites and S. alterniflora

We found the native *S. alterniflora* attenuated waves more effectively than *Phragmites* during more common inundation conditions (water level = 0.75 m) and with equal effectiveness during more extreme conditions (water level = 1.4 m and 2.0 m). *Spartina alterniflora* grows at denser concentrations than *Phragmites*, so it is therefore expected that it would outperform the latter during times when neither plant species is completely submerged. However, the ability of a plant species to attenuate waves decreases significantly when the water level is above the stem height (e.g., the plants are submerged), and continues to decrease as the ratio between water level and stem height increases (Gedan et al. 2011; Anderson and Smith 2014). In our numerical simulations, *S. alterniflora* was submerged under the greater two water levels (1.4 m and 2.0 m) and *Phragmites* was only submerged under the greatest water level (2.0 m). It is noteworthy then that *S. alterniflora* was able to attenuate waves as effectively as *Phragmites* despite having a greater ratio of water level to stem height. Even under water levels ($\geq$ 2.0 m) and wave heights ($\geq$ 1.0 m) that exceed what would be expected at the site, *S. alterniflora* performs as well as *Phragmites* (Fig. 7, Supplemental Fig. 2). It appears that the greater density of *S. alterniflora* compensates for the lower stem height and allows the native plant to attenuate waves similarly to the taller, sparser *Phragmites*. One important caveat here is that the model does not account for plant morphology or stem flexibility, both of which can change seasonally. More work is needed to determine how differences between the two species in these parameters may affect their respective ability to attenuate waves.

Seasonal variation in the vegetation characteristics leads to seasonal variation in wave attenuation and the comparison between *Phragmites* and *S. alterniflora*. *Spartina alterniflora* attenuates waves more effectively later in the growing season (summer and fall) compared to the rest of the year (winter and spring). This is to be expected given the known effect of biomass on wave attenuation and agrees with previous work on a different *Spartina* species on the US Pacific Coast (Foster-Martinez et al. 2018). In their study, Foster-Martinez et al. (2018) found that wave attenuation by *S. foliosa* was so reduced during the winter, that waves grew while traveling over the corresponding portion of the marsh. In our study system, which features lower tide ranges and wave heights, both *S. alterniflora* and *Phragmites* maintained the ability to attenuate waves throughout the year. The timing of peak wave attenuation by *Phragmites* is slightly different than *S. alterniflora*, in that *Phragmites* attenuates slightly more in the spring than fall. Overall, the vegetation characteristics of *Phragmites* are less variable than those of *S. alterniflora* (Table 1). This is true within a given survey, as evidence by smaller confidence intervals (Figs. 6 and 7), and seasonally, as evidenced by smaller differences in wave attenuation from season to season (Fig. 6B–E). It is important to note that the model results are based on one to two surveys per season and that there was some offset between when the *Phragmites* and *S. alterniflora* marsh were surveyed. These results therefore offer a seasonal snapshot, but may not represent the average conditions for each season. Nevertheless, our vegetation measurements are comparable to other measurements in the Chesapeake Bay (see Anderson and Smith 2014; Garzon et al. 2019a; Ferreira et al. 2022).

Human development near the coast often depends on wetlands for protection from waves and storms (Barbier et al. 2011). Our work suggests that, under conditions that represent more typical windy or wavy days, *S. alterniflora* offers better protection than *Phragmites*. Furthermore, the period of the year that *S. alterniflora* outperforms *Phragmites* corresponds with hurricane season for the US Atlantic Coast. In other words, *S. alterniflora* offers the greatest level of protection over *Phragmites* when it is most needed by coastal communities. However, under conditions of storm surge or other high-water events, both plant species offer similar and reduced levels of protection. *Phragmites* invasion can therefore be associated with increased wave impacts on local communities under certain hydrodynamic conditions and times of the year. This study offers additional rationale for the management of this invasive species. It should be noted though, that while *Phragmites* attenuates waves less effectively than *S. alterniflora* under some conditions, it still attenuates waves much more effectively than bare sediment for a given topographical profile (Fig. 7). Removing *Phragmites* without the establishment of native species would result in a significantly greater wave hazard for local communities, under both common and extreme conditions. The most impactful management of invasive *Phragmites*—with regard to wave attenuation—must then also include the restoration of native vegetation.

Conclusion

Our long-term, high-temporal-resolution field monitoring confirms that invasive *Phragmites* attenuates waves. The magnitude of wave attenuation decreases for higher water levels and increases for higher wave height. Stem density is the vegetation characteristic with the strongest correlation to wave attenuation. Through numerical modeling, we found that native *S. alterniflora* vegetation is capable of greater wave attenuation than *Phragmites* outside of conditions representative of extreme storms. The comparison between the wave attenuation between the species exhibits a seasonal pattern, where *S. alterniflora* outperforms *Phragmites* the most during the fall, then summer. During higher water level and wave height conditions, and during the winter and spring, the two vegetation species performed similarly. Our work suggests that *Phragmites* invasion increases the wave hazard for local communities, but that the presence of a *Phragmites*-dominated marsh still offers more protection than bare sediment.

Supplementary Information The online version contains supplementary material available at https://doi.org/10.1007/s12237-022-01138-x.

Acknowledgements This work was funded by the National Oceanographic and Atmospheric Administration through the Ecological Effects of Sea Level Rise grant (EESLR grant NA19NOS4780179) by the National Centers for Coastal Ocean Science. We would like to thank G. Coelho, M. Henke, and M. Sniegowski for help in the field, A. de Souza de Lima for conversations that lead to the project development, and our EESLR partners at The Nature Conservancy (M. Canick and J. Specht) and Maryland Department of Natural Resources (N. Carlozo, R. Golden, and E. Campbell). Data are archived at https://doi.org/10.4211/hs.f7350813a1de4025a3b8e4d05284dc57 and https://doi.org/10.4211/hs.9034fa75324d46299984b681c54218e9.

Declarations

Competing Interests The authors declare no competing interests.

References

Anderson, M.E., and J.M. Smith. 2014. Wave attenuation by flexible, idealized salt marsh vegetation. *Coastal Engineering* 83: 82–92.

Angradi, T.R., S.M. Hagan, and K.W. Able. 2001. Vegetation type and the intertidal macroinvertebrate fauna of a brackish marsh: *Phragmites* vs *Spartina*. *Wetlands* 21 (1): 75–92.

Barbier, E.B., S.D. Hacker, C. Kennedy, E.W. Koch, A.C. Stier, and B.R. Silliman. 2011. The value of estuarine and coastal ecosystem services. *Ecological Monographs* 81 (2): 169–193.

Chambers, R.M., L.A. Meyerson, and K. Saltonstall. 1999. Expansion of Phragmites australis into tidal wetlands of North America. *Aquatic Botany* 64 (3–4): 261–273.

Chmura G.L., S.C. Anisfeld, D.R. Cahoon, and J.C. Lynch. 2003. Global carbon sequestration in tidal, saline wetland soils. *Global Biogeochemical Cycles* 17(4). https://doi.org/10.1029/2002GB001917.

Collins M., M. Sutherland, L. Bouwer, S.-M. Cheong, T. Frölicher, H. Jacot Des Combes, M. Koll Roxy, I. Losada, K. McInnes, B. Ratter, E. Rivera-Arriaga, R.D. Susanto, D. Swingedouw, and L. Tibig. 2019. Extremes, abrupt changes and managing risk. In: IPCC Special report on the ocean and cryosphere in a changing climate [H.-O. Pörtner, D.C. Roberts, V. Masson-Delmotte, P. Zhai, M. Tignor, E. Poloczanska, K. Mintenbeck, A. Alegría, M. Nicolai, A. Okem, J. Petzold, B. Rama, N.M. Weyer (eds.)] United Nations, 589–655.

Daly, C., D. Roelvink, A. van Dongeren, J.V.T. de Vries, and R. McCall. 2012. Validation of an advective-deterministic approach to short wave breaking in a surf-beat model. *Coastal Engineering* 60: 69–83.

Deegan L.A., J.E. Hughes, and R.A. Rountree. 2002. Salt marsh ecosystem support of marine transient species. In: Weinstein M.P., Kreeger D.A. (eds) Concepts and controversies in tidal marsh ecology. Springer, Dordrecht 333–365. https://doi.org/10.1007/0-306-47534-0_16

Ferreira, C., D. Bentley, A. Bigalbal, J. Haddad, J.L.G. Hervas, A. Khalid, P. Khanal, L. Kellar, B. Lanza, S. Lawler, A. de Lima, E. Paquier, T.W. Miesse, A. Vecchio, and A.M. Rezaie. 2022. Storm surges, waves, hydrodynamics and vegetation surveys in eastern shore of Virginia National Wildlife Refuge, VA, USA (2014–2017). *HydroShare*. https://doi.org/10.4211/hs.b6d0ade225af4a3388e8bdb01f586c6c.

Foster-Martinez, M.R., J.R. Lacy, M.C. Ferner, and E.A. Variano. 2018. Wave attenuation across a tidal marsh in San Francisco Bay. *Coastal Engineering* 136: 26–40.

Garzon, J.L., T. Miesse, and C.M. Ferreira. 2019a. Field-based numerical model investigation of wave propagation across marshes in the Chesapeake Bay under storm conditions. *Coastal Engineering* 146: 32–46.

Garzon, J.L., M. Maza, C.M. Ferreira, J.L. Lara, and I.J. Losada. 2019b. Wave attenuation by Spartina saltmarshes in the Chesapeake Bay under storm surge conditions. *Journal of Geophysical Research: Oceans* 124 (7): 5220–5243.

Gedan, K.B., M.L. Kirwan, E. Wolanski, E.B. Barbier, and B.R. Silliman. 2011. The present and future role of coastal wetland vegetation in protecting shorelines: Answering recent challenges to the paradigm. *Climatic Change* 106 (1): 7–29.

Glass, E.M., J.L. Garzon, S. Lawler, E. Paquier, and C.M. Ferreira. 2018. Potential of marshes to attenuate storm surge water level in the Chesapeake Bay. *Limnology and Oceanography* 63 (2): 951–967.

Langston, A.K., D.J. Coleman, N.W. Jung, J.L. Shawler, A.J. Smith, B.L. Williams, S. Wittyngham, R.M. Chambers, J.E. Perry, and M.L. Kirwan. 2021. The effect of marsh age on ecosystem function in a rapidly transgressing marsh. *Ecosystems* 25 (2): 252–264.

Loder, N.M., J.L. Irish, M.A. Cialone, and T.V. Wamsley. 2009. Sensitivity of hurricane surge to morphological parameters of coastal wetlands. *Estuarine, Coastal and Shelf Science* 84 (4): 625–636.

Massel, S.R., K. Furukawa, and R.M. Brinkman. 1999. Surface wave propagation in mangrove forests. *Fluid Dynamics Research* 24 (4): 219–249.

Maza, M., J.L. Lara, I.J. Losada, B. Ondiviela, J. Trinogga, and T.J. Bouma. 2015. Large-scale 3-D experiments of wave and current interaction with real vegetation. Part 2: Experimental analysis. *Coastal Engineering* 106: 73–86.

Meyer, S.W., S.S. Badzinski, S.A. Petrie, and C.D. Ankney. 2010. Seasonal abundance and species richness of birds in common reed habitats in Lake Erie. *The Journal of Wildlife Management* 74 (7): 1559–1566.

Möller, I., M. Kudella, F. Rupprecht, T. Spencer, M. Paul, B.K. van Wesenbeeck, G. Wolters, K. Jensen, T.J. Bouma, M. Miranda-Lange, and S. Schimmels. 2014. Wave attenuation over coastal salt marshes under storm surge conditions. *Nature Geoscience* 7: 727–731. https://doi.org/10.1038/ngeo2251.

Norris, K., P.W. Atkinson, and J.A. Gill. 2004. Climate change and coastal waterbird populations–past declines and future impacts. *Ibis* 146: 82–89.

Paquier, A.E., J. Haddad, S. Lawler, and C.M. Ferreira. 2017. Quantification of the attenuation of storm surge components by a coastal wetland of the US Mid Atlantic. *Estuaries and Coasts* 40: 930–946. https://doi.org/10.1007/s12237-016-0190-1.

Roelvink, D., A. Reniers, A.P. Van Dongeren, J.V.T. De Vries, R. McCall, and J. Lescinski. 2009. Modelling storm impacts on beaches, dunes and barrier islands. *Coastal Engineering* 56 (11–12): 1133–1152.

Rooth, J.E., and J.C. Stevenson. 2000. Sediment deposition patterns in *Phragmites australis* communities: Implications for coastal areas threatened by rising sea-level. *Wetlands Ecology and Management* 8 (2): 173–183.

Rooth, J.E., J.C. Stevenson, and J.C. Cornwell. 2003. Increased sediment accretion rates following invasion by *Phragmites australis*: The role of litter. *Estuaries* 26 (2): 475–483.

Saltonstall, K. 2002. Cryptic invasion by a non-native genotype of the common reed, *Phragmites australis*, into North America. *Proceedings of the National Academy of Sciences* 99 (4): 2445–2449.

Sheng, Y.P., A.A. Rivera-Nieves, R. Zou, V.A. Paramygin, C. Angelini, and S.J. Sharp. 2021. Invasive *Phragmites* provides superior wave and surge damage protection relative to native plants during storms. *Environmental Research Letters* 16 (5): 054008.

Silliman, B.R., and M.D. Bertness. 2004. Shoreline development drives invasion of *Phragmites australis* and the loss of plant diversity on New England salt marshes. *Conservation Biology* 18 (5): 1424–1434.

Van Rooijen A.A., J.S.M. Van Thiel de Vries, R.T. McCall, A.R. Van Dongeren, J.A. Roelvink,, and A.J.H.M. Reniers. 2015. Modeling of wave attenuation by vegetation with Xbeach. In *E-proceedings of the 36th IAHR World Congress, The Hague, the Netherlands, 28 June-3 July 2015*. IAHR., The Hague, Netherlands. 1–7.

Vuik, V., S.N. Jonkman, B.W. Borsje, and T. Suzuki. 2016. Nature-based flood protection: The efficiency of vegetated foreshores for reducing wave loads on coastal dikes. *Coastal Engineering* 116: 42–56.

Weinstein, M.P., and J.H. Balletto. 1999. Does the common reed, *Phragmites australis*, affect essential fish habitat? *Estuaries* 22 (3): 793–802.

Windham, L., J.S. Weis, and P. Weis. 2003. Uptake and distribution of metals in two dominant salt marsh macrophytes, *Spartina alterniflora* (cordgrass) and *Phragmites australis* (common reed). *Estuarine, Coastal and Shelf Science* 56 (1): 63–72.

Xue, L., X. Li, B. Shi, B. Yang, S. Lin, Y. Yuan, Y. Ma, and Z. Peng. 2021. Pattern-regulated wave attenuation by salt marshes in the Yangtze Estuary, China. *Ocean & Coastal Management* 209: 105686–105670.